Densification kinetics of MnO-doped UO$_2$-10 wt%Gd$_2$O$_3$ compact

Young Woo Rhee [*], Keon Sik Kim, Kun Woo Song

Advanced PWR Fuel Development Division, Korea Atomic Energy Research Institute, Daejon 305-353, Republic of Korea

Available online 1 December 2006

Abstract

The effect of MnO doping on the densification behavior of the UO$_2$-10 wt%Gd$_2$O$_3$ compact has been investigated by using a high-temperature pushrod dilatometer up to 1650 °C. Dilatometry results show that small amounts of MnO enhance the sintering of the UO$_2$-10 wt%Gd$_2$O$_3$ compact leading to a very high densification rate at low temperatures of about 1250 °C. The sintered density substantially was increased by more than 1% of the theoretical density in only 0.01 wt% of MnO added sample. A small amount of MnO also promotes the grain growth dramatically. The UO$_2$-10 wt%Gd$_2$O$_3$ pellet with 0.1 wt% of MnO shows a 2.5 times larger grain size than the undoped UO$_2$-10 wt%Gd$_2$O$_3$ pellet. These results might be attributed to the enhanced grain boundary mobility, which probably resulted from a large distortion of the surrounding lattice.

© 2006 Elsevier B.V. All rights reserved.

Keywords: Sintering; Burnable Absorber; Nuclear fuel

1. Introduction

Gadolinia has been employed as a burnable absorber, UO$_2$-Gd$_2$O$_3$ fuel pellets, to suppress the initial excess reactivity at the beginning of life in a light water reactor. The UO$_2$-Gd$_2$O$_3$ pellets are fabricated in a similar way with that of the UO$_2$ pellets because most of the processes are based on the commercial UO$_2$ pellet fabrication method [1]. However, the UO$_2$-Gd$_2$O$_3$ pellet is more difficult to fabricate than the UO$_2$ pellet because of its smaller grain size and poor homogeneity of the UO$_2$-Gd$_2$O$_3$ solid solution under the same sintering temperature and atmosphere.

The sintering behavior and the microstructure of a sintered UO$_2$-Gd$_2$O$_3$ pellet are considerably influenced by the mixing condition of UO$_2$ and Gd$_2$O$_3$, the oxygen potential of the sintering atmosphere and the sintering additives. Riella et al. [2] reported that the UO$_2$-Gd$_2$O$_3$ pellet using co-precipitated (U,Gd)O$_2$ powder showed a better homogenous Gd distribution than that made by any other mixing method. There have been some studies [3–5] on the effect of the sintering atmosphere on the properties of the UO$_2$-Gd$_2$O$_3$ pellets. They have reported that the sintered density decreases as the oxygen potential of the sintering atmosphere increases.

Some researchers [1,6,7] have studied the effects of sintering additives such as Al$_2$O$_3$, TiO$_2$, and Cr$_2$O$_3$-SiO. Assmann et al. [1] showed that a simply mixed UO$_2$-Gd$_2$O$_3$ powder was able to be sintered up to 95% TD by adding Al$_2$O$_3$. It is reported that Al(OH)$_3$ and TiO$_2$ have a beneficial effect on the densification of the UO$_2$-Gd$_2$O$_3$ pellets [6]. Kim et al. [7] have investigated the role of a composite additive, Cr$_2$O$_3$-SiO$_2$, and they also observed an enhanced densification of the UO$_2$-Gd$_2$O$_3$ pellets. All the above additives increased the sintered density after a final-stage sintering. However, it seems that they have a little effect on the initial- or the intermediate-stage densification.

The Gd$_2$O$_3$ contents of the UO$_2$-Gd$_2$O$_3$ pellets are usually in the range of 4–8 wt%. However, the content of Gd$_2$O$_3$ tends to become higher with an extension of the fuel cycle length. It is known that high Gd$_2$O$_3$ contents are apt to decrease the sintered density and grain size of UO$_2$-Gd$_2$O$_3$ pellets. The present study has been undertaken to improve the density and grain size of the UO$_2$-Gd$_2$O$_3$ pellet with high Gd$_2$O$_3$ contents by using a new sintering additive, MnO. There are few reports on the effect of MnO on the sintering of the UO$_2$ or UO$_2$-Gd$_2$O$_3$ pellets. Recently, it was reported that MnO-SiO$_2$ causes a considerable enhancement in the grain growth of the UO$_2$ pellet [8]. The effect of MnO on the sintering and densification kinetics of the UO$_2$-Gd$_2$O$_3$ powder compact has been investigated.

[*] Corresponding author. Tel.: +82 42 868 2815; fax: +82 42 861 7340.
E-mail address: youngwoo@kaeri.re.kr (Y.W. Rhee).

2. Experimental procedures

2.1. Powder preparation

Samples were prepared from the ADU route UO_2, Gd_2O_3 (Aldrich, 99.9%) and MnO (Kosundo chemicals, 99.9% in purity) powders. A mixture of MnO and Gd_2O_3 powder was subjected to a ball milling for 12 h in ethyl alcohol using a polyethylene bottle and high purity zirconia balls to prepare a MnO-doped Gd_2O_3 powder. The dried slurry was screened in a 100 mesh sieve. The powder thus prepared was mixed with UO_2 powder in a tumbling mixer for 1 h, and it was then pulverized in a pestle and mortar for 10 min to prepare a MnO-doped UO_2-10 wt%Gd_2O_3 powder. The contents of MnO were 0.01, 0.02, 0.05, and 0.1 wt%. Undoped UO_2-10 wt%Gd_2O_3 powder was prepared following the same procedure as the MnO-doped powder without a MnO addition. UO_2-1 wt%MnO and Gd_2O_3-1 wt%MnO powders for the phase analysis were also prepared by following the above procedure.

2.2. Dilatometry and microstructural observation

The prepared powder was pressed under 3 ton/cm^2 into cylindrical powder compacts of about 8 mm in diameter and about 10 mm in height. The green densities of the compacts were around 50% of the theoretical density. The shrinkage of the compacts was measured up to 1650 °C in H_2-3%CO_2 by using a push rod type dilatometer (Netzsch, Dil402C). For a microstructural observation, the powder was pressed under 3 ton/cm^2 into cylindrical compacts of about 10 mm in diameter and about 10 mm in height. The compact was heated to 1730 °C at a rate of 5 K/min, and it was then sintered for 4 h in H_2-3% CO_2. UO_2-1 wt%MnO and Gd_2O_3-1 wt%MnO powders were compacted under 3 ton/cm^2 and then sintered at 1000, 1200 and 1500 °C for 1 h in H_2-3% CO_2 for the phase analysis. The sintered density was measured by using the water immersion method. The microstructure was determined by an optical microscope and a scanning electron microscope before and after being thermally etched at 1250 °C for 1 h in CO_2. Energy dispersive spectroscopy (EDS) analysis was preformed on the polished surfaces of the sintered samples.

3. Results and discussion

The phase stability of MnO in the reductive sintering atmosphere, H_2-3% CO_2, was estimated by using the SOLGASMIX program [9], which can calculate the Gibbs free energy and equilibrium constant of a reaction. The calculated results under a total gas pressure of 1 bar are plotted against the temperature in Fig. 1. The line 1 and the line 2 indicate the oxygen potential ($\Delta \bar{G}_{O_2} = RT \ln p_{O_2}$) of MnO and that of the sintering atmosphere, H_2-3% CO_2, respectively. MnO is the stable phase above the line 1 and manganese is stable below the line 1. The line 2 lies above the line 1 for the whole temperature ranges. It suggests that MnO does not reduce to a metallic form for the whole sintering schedule. Manganese remains as an oxide form, which is more easily soluble in UO_2 and Gd_2O_3.
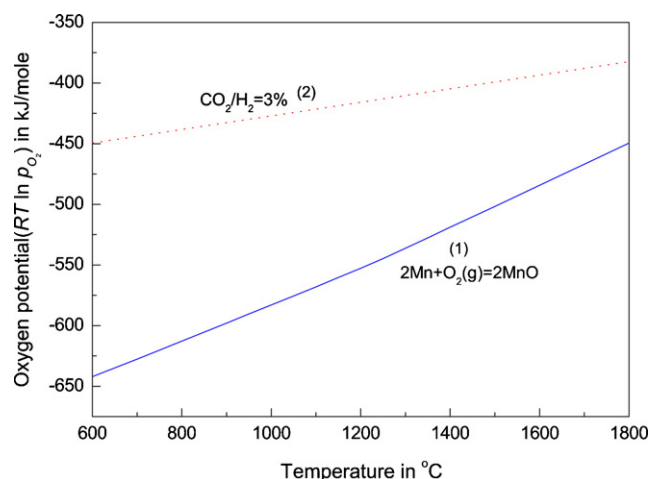

Fig. 1. Oxygen potentials of the MnO and sintering gas as a function of the temperature.

Fig. 2 shows the shrinkage curves and the shrinkage rates as a function of the temperature for the compacts with various MnO contents. It appears that the addition of MnO shifts both the shrinkage curve (Fig. 2(a)) and the temperature of the maximum shrinkage rate (Fig. 2(b)) toward the left, the lower temperature
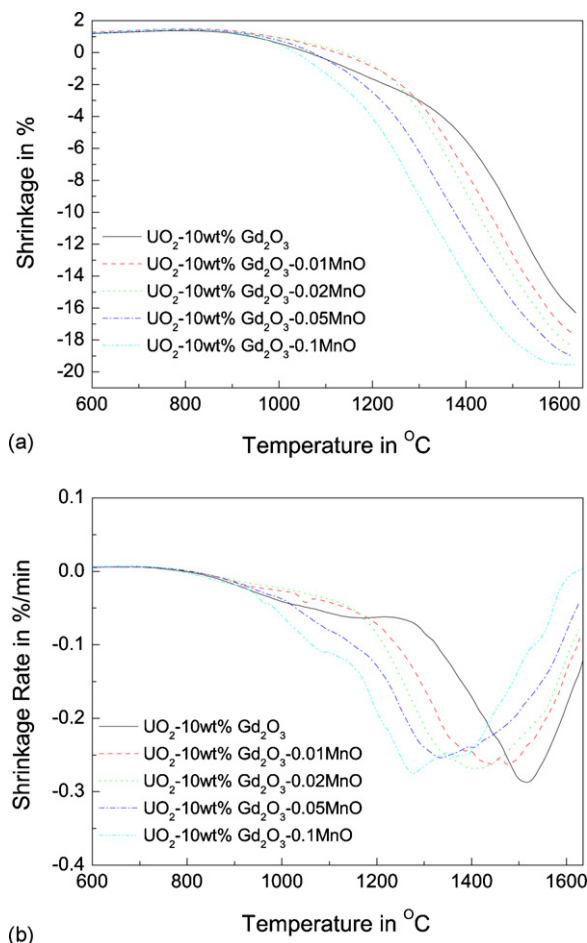

(a)

(b)

Fig. 2. Shrinkage curves and shrinkage rates as a function of the temperature for various MnO contents.
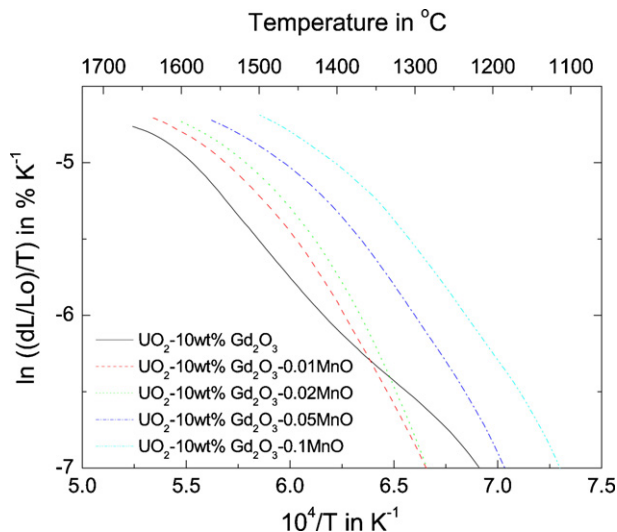
Fig. 3. $\ln((dL/L_0)/T)$ vs. $1/T$ for various MnO contents.

Fig. 4. Sintered density of the UO$_2$-10 wt%Gd$_2$O$_3$ pellets with various MnO contents.

region. The temperature of the maximum shrinkage rate shifts from 1520 °C for the undoped UO$_2$-10 wt%Gd$_2$O$_3$ to 1260 °C for the 0.1% MnO-doped one. The magnitudes of the shifts in the shrinkage curve and the temperature of the maximum shrinkage rate increase with the content of MnO. These results suggest that the addition of MnO appears to have a considerable effect on the initial- or the intermediate-stage densification.

Young and Cutler [10] developed an equation for an initial-stage sintering under a constant heating rate condition as follows:

$$\frac{(\Delta L/L_0)}{T} = A \exp\left[-\frac{Q}{(m+1)RT}\right] \tag{1}$$

where, $\Delta L/L_0$ is the relative length change, T the temperature. A is a constant depending only on the materials parameters and the sintering mechanisms. The exponent, m, have values of 0 for a
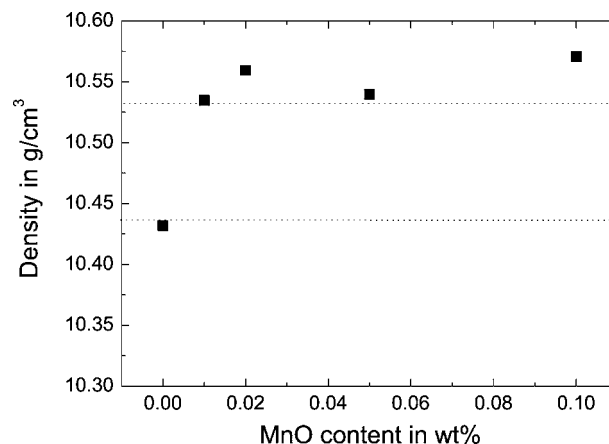
viscous flow, 1 for a volume diffusion and 2 for a grain boundary diffusion mechanism. Based on Eq. (1), $\ln[(\Delta L/L_0)/T]$ versus $1/T$ at a heating rate of 5 K/min is plotted in Fig. 3. If the value of m is known, the apparent activation energy, Q, could be estimated from the slope of the plots in Fig. 3.

In the case of an undoped UO$_2$-10 wt%Gd$_2$O$_3$, it seems to have two linear parts of different slopes in the vicinity of 1400 °C. The lower slope in the temperatures between 1200 and 1400 °C may be attributed to a delay of the densification of an undoped UO$_2$-10 wt%Gd$_2$O$_3$ compact. It is known that a delay of the densification is associated with the formation of a (U,Gd)O$_2$ solid solution [11].

MnO-doped UO$_2$-10 wt%Gd$_2$O$_3$ compacts appear to have one linear part for each contents of MnO and they have a different initial-stage sintering mechanism from the undoped one. The slopes of the MnO-doped UO$_2$-10 wt%Gd$_2$O$_3$ compacts seem to decrease with increasing MnO contents. Assuming
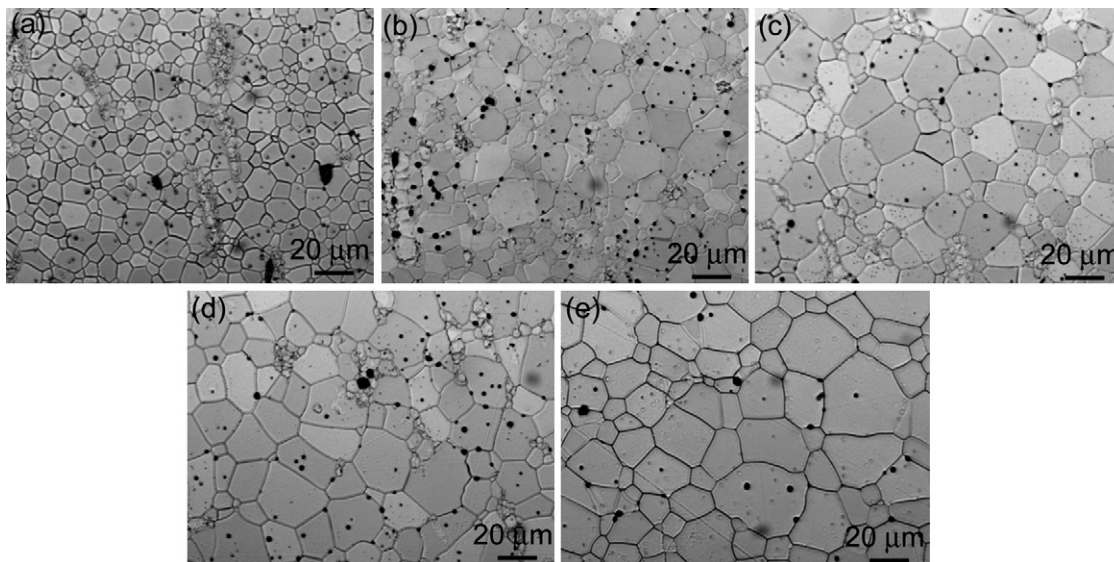

Fig. 5. Microstructures of the undoped and doped UO$_2$-10 wt%Gd$_2$O$_3$ pellets sintered at 1730 °C for 4 h; (a) undoped, (b) 0.01% MnO, (c) 0.02%, (d) 0.05%, (e) 0.1%.
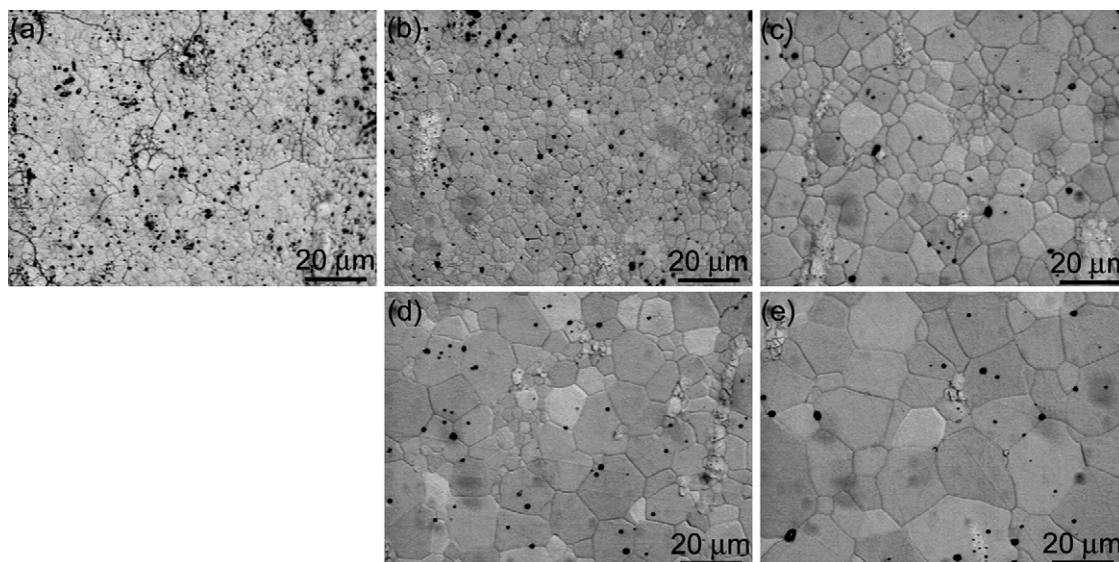
Fig. 6. Microstructures of the undoped and doped UO_2-10 wt%Gd_2O_3 pellets sintered at 1630 °C for 4 h; (a) undoped, (b) 0.01% MnO, (c) 0.02%, (d) 0.05%, (e) 0.1%.

that all the MnO-doped UO_2-10 wt%Gd_2O_3 compacts have the same initial-stage sintering mechanism, the apparent activation energy appears to decrease with increasing MnO contents. For the case of $m = 1$ (volume diffusion), the activation energies for the MnO-doped UO_2-10 wt%Gd_2O_3 compacts were estimated 54300, 46300, 31500 and 21200 cal/mole with increasing the MnO contents from 0.01 to 0.1 wt%. Those values are lower than the activation energy of the undoped UO_2-10 wt%Gd_2O_3 compact, 63900 cal/mole.

Fig. 4 shows the effect of the MnO contents on the sintered density of the UO_2-10 wt%Gd_2O_3 pellet sintered at 1730 °C for 4 h in H_2-3%CO_2. It appears that the addition of only 0.01% MnO causes a significant increase in the sintered density. It is also seen that an additive content greater than 0.01% has little effect on a further densification.

The grain structures of the UO_2-10 wt%Gd_2O_3 pellet sintered at 1730 °C for 4 h in H_2-3%CO_2 are shown in Fig. 5. The grain size of the undoped UO_2-10 wt%Gd_2O_3 pellet is about 9 μm. Those of the MnO-doped UO_2-10 wt%Gd_2O_3 pellets increased with an increasing MnO content. That of the 0.1% MnO-doped UO_2-10 wt%Gd_2O_3 pellet increases up to about 23 μm. Some clusters of small grains can be seen in Fig. 5(a–d). Kim et al. [7] reported that this cluster was the Gd deficient region. The area fraction of the small-grained cluster decreases with an increasing MnO content and then the cluster disappears in the 0.1% MnO-doped sample.

All the results presented so far suggest that the addition of MnO could decrease significantly the sintering temperature of the UO_2-10 wt%Gd_2O_3 pellet. An example of which can be seen in Fig. 6. The sintering temperature of the samples in Fig. 6 is lower than that of the samples in Fig. 5 by 100 °C. Fig. 6 shows the grain structures of the UO_2-10 wt%Gd_2O_3 pellet sintered at 1630 °C for 4 h in H_2-3%CO_2. Even though the sintering temperature is lower by 100 °C, it appears to have high densities and similar relationships between the density and the MnO content.

The addition of only 0.01% MnO causes a significant increase in the pore shrinkage. It is also seen that an additive content greater than 0.01% has a little effect on a further densification. However, the grain sizes in Fig. 6 are smaller than those in Fig. 5 by about 30%.

Manganese appears to result in an enhanced promotion of the densification in separate UO_2 and Gd_2O_3 pellets. The sintered density of the UO_2-1 wt%MnO and Gd_2O_3-1 wt%MnO pellets as a function of the sintering temperature is shown in Fig. 7. All the samples are sintered at each temperature for 1 h in H_2-3% CO_2 and then quenched to room temperature. The addition of MnO causes a significant increase in the sintered density of UO_2 and Gd_2O_3. These samples were almost fully densified at 1200 °C, even in a very low temperature and short sintering time. It is also seen that the dedensification occurs in both cases at 1500 °C.
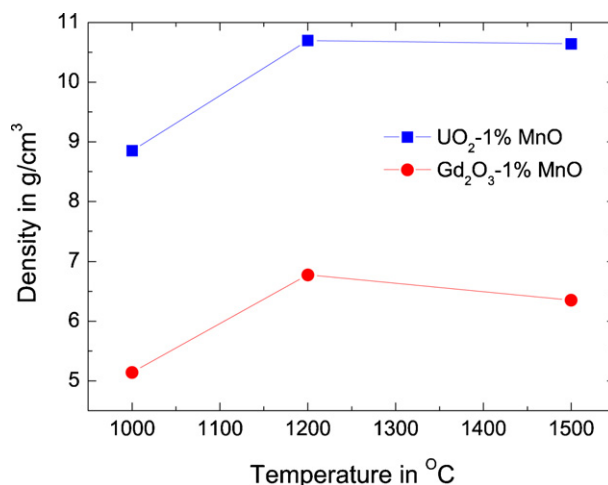

Fig. 7. Sintered density of the UO_2-1 wt%MnO and Gd_2O_3-1 wt%MnO pellets after a sintering at the various temperatures.
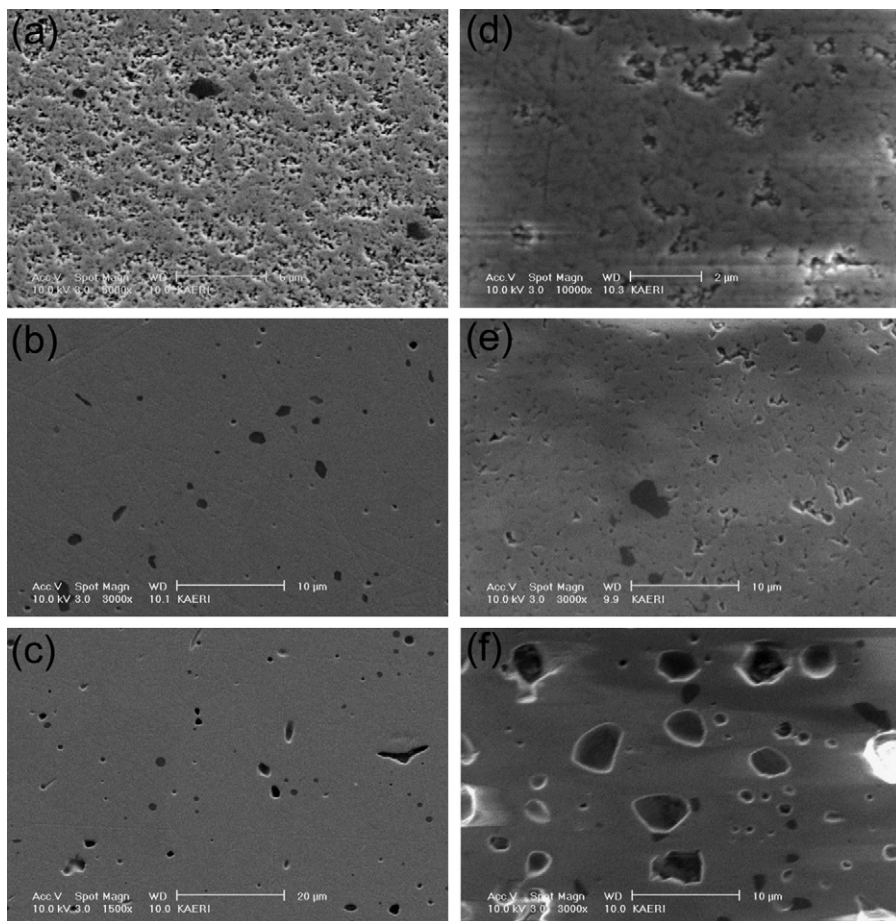
Fig. 8. Pore structures of the UO$_2$-1 wt%MnO (a–c) and Gd$_2$O$_3$-1 wt%MnO (d–f) pellets after a sintering at the various temperatures; (a, d) 1000 °C, (b, e) 1200 °C, (c, f) 1500 °C.

Fig. 8 shows the pore structures of the UO$_2$-1 wt%MnO and Gd$_2$O$_3$-1 wt%MnO pellets in Fig. 7. The pore structures are consistent with the results of the sintered densities in Fig. 7. Dark black precipitates were easily found in the polished surfaces. The EDS analysis shows that the composition of the precipitates was mainly composed of manganese ($\sim$72 at%) and oxygen ($\sim$28 at%).

Zhang et al. [12] observed a similar promotion of a densification and grain growth in transient metal-doped CeO$_2$. They suggested that this promotion may be attributed to the effect of the severe ionic size difference between the dopant and the matrix ions. Chen et al. [13] suggested that severely undersized dopants have a tendency to enhance the grain boundary mobility due to a large distortion of the surrounding lattice that facilitates a defect migration of the matrix. The ionic size of manganese is much smaller than that of uranium or gadolinium. Thus, a similar interpretation could be appropriate to the present investigation. Mn ions in the UO$_2$-Gd$_2$O$_3$ pellet have a severely undersized ionic size, much more than that of the UO$_2$-Gd$_2$O$_3$ matrix and thus may enhance the grain boundary mobility due to a large distortion of the surrounding lattice. Further studies are needed to establish the mechanism of an enhanced densification in an early-stage sintering and the promoted grain growth in the MnO-doped UO$_2$-Gd$_2$O$_3$ pellet.

4. Conclusion

MnO doping in the UO$_2$-10 wt%Gd$_2$O$_3$ system accelerates a thermally activated material transport, so the onset of a densification as well as the temperature of the maximum densification rate shift to the lower temperature region. Within the studied doping level, from 0.01 to 0.1 wt%, the content of MnO has a significant effect on the densification behavior and grain growth of the UO$_2$-10 wt%Gd$_2$O$_3$ pellet. Dilatometry results and microstructural observation confirm that the 0.1 wt%MnO doping could reduce the sintering temperature by more than 100 °C and it enhances the grain growth.

References

[1] H. Assmann, M. Peehs, H. Roepenack, J. Nucl. Mater. 153 (1988) 115.
[2] H.G. Riella, M. Durazzo, M. Hirata, R.A. Nogueira, J. Nucl. Mater. 178 (1991) 204.

[3] S.M. Ho, K.C. Radfod, Nucl. Technol. 73 (1986) 350.
[4] R. Yuda, K. Une, J. Nucl. Mater. 178 (1991) 195.
[5] K.W. Song, K.S. Kim, Y.S. Yoo, Y.H. Jung, J. Kor. Nucl. Soc. 30 (1998) 128.
[6] K.W. Kang, K.S. Kim, K.W. Song, J.H. Yang, Y.H. Jung, J. Kor. Nucl. Soc. 32 (2000) 559.
[7] K.S. Kim, K.W. Song, K.W. Kang, J.H. Yang, J.H. Kim, J. Kor. Nucl. Soc. 33 (2001) 386.
[8] Y.W. Rhee, K.W. Kang, K.S. Kim, J.H. Yang, J.H. Kim, K.W. Song, Nucl. Eng. Technol. 37 (2005) 287.
[9] HSC Chemistry for Windows, Outokump Research, 1994.
[10] W.S. Young, I.B. Cutler, J. Am. Ceram. Soc. 53 (1970) 659.
[11] R. Manzel, W.O. Doerr, Am. Ceram. Soc. Bull. 59 (1980) 601.
[12] T. Zhang, P. Hing, H. Huang, J. Kilner, J. Eur. Ceram. Soc. 22 (2002) 27.
[13] P.-L. Chen, I.-W. Chen, J. Am. Ceram. Soc. 79 (1996) 1793.